Mode switching torque distribution strategy of timely four-wheel driven high-gap plant protection machine

Haijun Zhang[1], Mingwei Guan[1], Guojun Ji[2], Ghulam Hussain[3], Maohua Xiao[1], Yejun Zhu[1*]

(1. *College of Engineering, Nanjing Agricultural University, Nanjing 210031, China*;
2. *Essen Agricultural Machinery Changzhou Co., Ltd., Changzhou 213000, China*;
3. *Faculty of Mechanical Engineering, Ghulam Ishaq Khan Institute of Engineering Sciences & Technology, Topi 23460, Pakistan*)

Abstract: The high-gap plant protection machine is taken in this paper as the research object to ensure the good driving power and safety of the high-gap plant protection machine, and the control strategy of inter-shaft torque distribution is established under different working conditions to improve vehicle power and lateral stability. The anticipated demand torque is initially determined based on the structural characteristics and operational principles of the plant protection machine. Subsequently, a hierarchical control framework is devised by incorporating a formulated switching control strategy. Finally, a simulation model for torque distribution control strategy between shafts is developed on the Matlab/Simulink platform, followed by simulation and experimental verification. The results are presented as follows: the inter-shaft torque distribution strategy established in this paper increases the average longitudinal acceleration by 0.13 m/s^2 and 0.14 m/s^2 under the control of low and high to low adhesion road surfaces, respectively. Under the control of the single-line shifting condition, the yaw velocity can successfully follow the expected value with a maximum value of 0.61 rad/s. The side deflection angle of the center of mass does not exceed 2.8°, which can follow the ideal trajectory and improve power and safety.

Keywords: plant protection robot, torque distribution, mode switching
DOI: 10.25165/j.ijabe.20241704.8752

Citation: Zhang H J, Guan M W, Ji G J, Hussain G, Xiao M H, Zhu Y J. Mode switching torque distribution strategy of timely four-wheel driven high-gap plant protection machine. Int J Agric & Biol Eng, 2024; 17(4): 176–184.

1 Introduction

In modern agriculture, the efficiency and reliability of agricultural machinery are crucial for enhancing crop yield and quality[1]. Particularly in field environments, upland clearance planting machines encounter challenges such as poor traveling stability and a high rate of seedling injury due to fluctuating road conditions[2]. In the face of these complex and diverse operating environments, an accurate torque distribution system can ensure the stable operation of plantation protection machines under various working conditions, thereby enhancing operational efficiency[3,4]. Therefore, rational torque distribution not only ensures operational quality and improves crop protection effectiveness but also enhances operational safety and mitigates potential risks[5-7]. Current research of domestic and foreign experts on torque distribution and driving mode switching mainly focuses on electric vehicles[8]. Li et al.[9] proposed an optimal torque distribution method for electric vehicles equipped with four independent wheel motors to improve vehicle controllability and stability. Dizqah et al.[10] indicated that the optimal torque distribution was formulated as a solution to the parameter optimization problem, which can save a considerable amount of energy compared with the traditional torque distribution strategy. Cao et al.[11] introduced a multi-objective optimal torque distribution strategy considering the changes in load transfer and adhesion characteristics of the front and rear axles. Yan et al.[12] proposed a hybrid four-wheel driven tractor and developed a torque distribution control strategy based on fuzzy control. Peng et al.[13] adopted fuzzy recognition to identify the driver's intention and developed different torque distribution control strategies for various intentions.

Analysis results of the above research content of domestic and foreign torque distribution strategies revealed that domestic and foreign scholars have conducted in-depth studies on the dynamic characteristics and torque distribution control strategies of various four-wheel driven vehicles under straight-line and turning conditions. However, most of these control strategies are based on the inter-wheel torque distribution control approaches established by electric four-wheel driven vehicles[14]. Moreover, the control strategy of torque distribution between shafts under multiple working conditions is rarely studied, and in-depth research is needed[15].

This paper will start from the inter-shaft torque distribution device of the timely four-wheel driven system of the high-clearance plant protection machine and analyze its structure and working principle of each component. The dynamic characteristics of the vehicle under dynamic operation are obtained, and the appropriate driving mode is selected in accordance with different working conditions to improve the power and safety of the vehicle[16,17]. The target torque in the high-efficiency range is taken as the multidrive mode switching point based on the timely four-wheel driven system of the high-gap plant protection machine[18]. Compared with the load torque, the vehicle must overcome under a certain working condition, the drive mode selection and switching are conducted,

Received date: 2023-12-27 **Accepted date:** 2024-05-07
Biographies: Haijun Zhang, Associate Professor, research interest: intelligent agricultural machinery, Email: zhhj@njau.edu.cn; **Mingwei Guan**, MS, research interest: intelligent agricultural machinery, Email: 2022812080@stu.njau.edu.cn; **Guojun Ji**, MS, research interest: intelligent agricultural machinery, Email: jx9816@163.com; **Ghulam Hussain**, Professor, research interest: intelligent agricultural machinery, Email: gh_ghumman@hotmail.com; **Maohua Xiao**, Professor, research interest: intelligent agricultural machinery, Email: xiaomaohua@njau.edu.cn.
***Corresponding author: Yejun Zhu**, PhD, Lecturer, research interest: intelligent agricultural machinery. No.40, Dianjiangtai Road, Pukou District, Nanjing 210031, China. Tel: +86-15250952212, Email: yjzhu@njau.edu.cn.

and the torque is optimized to improve the utilization of power and safety[19].

2 Vehicle chassis drive system

A timely four-wheel driven system is adopted by the high-gap sprayer based on the rear-drive vehicle, as shown in Figure 1. The main driving wheel is the rear wheel, the longitudinal form is held by the engine in front, and the transmission output and rear shafts are connected with the front shaft through the inter-shaft clutch device. Thus, the steering bridge is sufficiently shaped into a wide structural form by the sprayer[20]. The steering structure of the high-gap sprayer is constituted by the front and rear steering bridge, the spray locomotive wheel, and the main body of the frame. A special tread design of paddy field is adopted by the spray locomotive wheel[21], which can effectively improve the wheel grip in the field. The same structure is observed in the front and rear steering bridges, which include a supporting bridge and a rotating support device. The rigid body of the fully welded door is mainly found in the steering bridge. The rigidity of the steering bridge and the adaptability of the sprayer to the environment are both optimized by the aforementioned structural design[22].

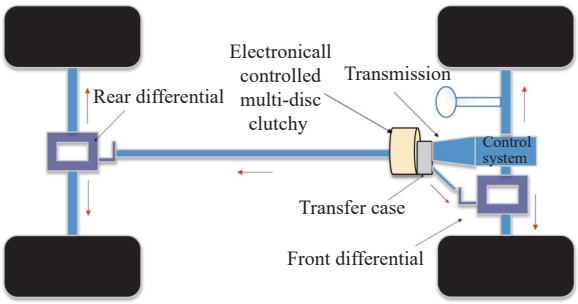

Figure 1 Structural diagram of the timely four-wheel driven chassis drive train

The speed ratios of the front and rear shaft reducers are i_f and i_r, respectively. These reducers mainly aim to change the direction of torque transmission while slowing down and increasing torque[23]. The torque distribution device can achieve the locking function by meeting the following requirements:

$$i_f = i_r \tag{1}$$

Different driving states for the timely four-wheel driven system studied in this paper are required under various working conditions. The rear-drive mode is indicated by driving on a good road surface. Vehicle turning and trapping are facilitated by the road surface with a low adhesion coefficient[24]. The vehicle drive is created in accordance with the necessary special conditions to effectively use the output power of the engine and maintain good power and stability[25]. The rear-drive mode is then switched to the four-wheel-drive mode to help the front wheels obtain some power[26].

3 Torque distribution control method

3.1 Demand torque analysis of timely four-wheel driven system

In the actual vehicle, the vehicle speed is controlled by the driver through the accelerator and brake pedals, and the necessary energy to meet the torque demand of the driver is addressed by the energy management controller. The speed is constantly changed according to the input/output torque of the power components[27]. In addition, the driver's required torque is predicted by a combination of factors such as accelerator pedal opening/opening rate of change. Based on the above advantages, the relationship between the driver's demand torque and speed can be transformed using the vehicle longitudinal dynamics equation[28,29]. The vehicle longitudinal dynamics is used to obtain the longitudinal speed of the vehicle as follows:

$$M\dot{V} = T_{mot} i_g(\gamma) i_0 \eta_t / R_W - F_b - F_r, \tag{2}$$

where, M is the maintenance mass, kg; T_{mot} is the engine torque, N·m; γ is the transmission gear, i_g is the transmission ratio corresponding to the gear; η_t is the mechanical transmission efficiency; i_0 is the transmission ratio of the main reducer; R_W is the wheel radius, m; F_b is the braking force, N; F_r is the sum of the driving resistance, N.

The demand torque of the driver is finally predicted. The exponential function prediction formula is as follows:

$$T_{\text{req}}(k+i) = T_{\text{req}}(k)\exp(-i/T_d)\ i = 1,2,\ldots,T_p \tag{3}$$

where, $T_{\text{req}}(k+i)$, which is the required torque at time k+1, is predicted for time k, N·m; T_d is the decay factor of the exponential function.

Root mean square error is selected as the evaluation index to determine the accuracy of torque prediction, and the expression is

$$R(k) = \sqrt{\sum_{i=1}^{T_P} (T_{\text{req}}^{\text{act}}(k+i) - T_{\text{req}}^{\text{ref}}(k+i)^2)/T_p} \tag{4}$$

$$Re = \sqrt{\sum_{k=1}^{L} R^2(k)/L} \tag{5}$$

where, $R(k)$ is the root mean square error of torque in the time domain predicted at time k; $\boldsymbol{Re}$ is the root mean square error of torque in the entire cycle condition (a small prediction error indicates a high prediction accuracy); $T_{\text{req}}^{\text{ref}}(k+i)$ is the required torque at time k+1 predicted at time k, N·m; $T_{\text{req}}^{\text{act}}(k+i)$ is the actual demand torque at k+1 moment, N·m; $\boldsymbol{L}$ is the total step length of the cycle condition; and $\boldsymbol{T_p}$ is the predict step size.

Figure 2 shows the root mean square of torque error predicted based on exponential function. The figure reveals that $\boldsymbol{R_e}$ will continue to increase with $\boldsymbol{T_p}$ due to the irregular change in the driver's demand torque with the rise in the predicted step length, and the prediction accuracy decreases. In the same prediction time domain, increasing $\boldsymbol{R_e}$ can gradually reduce $\boldsymbol{T_d}$; however, with the increase in $\boldsymbol{T_d}$, the amplitude of $\boldsymbol{R_e}$ reduction will also decrease and gradually remain as a fixed value[30].

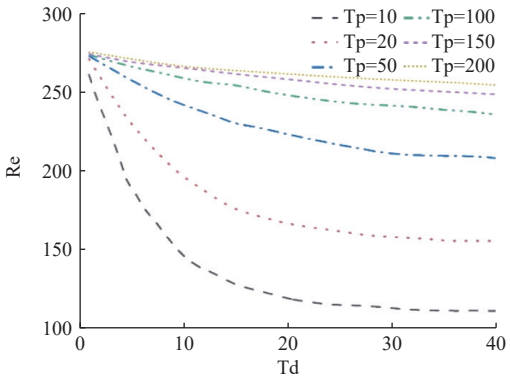

Figure 2 Prediction result of exponential function

The driving mode switching is mainly based on the size of the required torque A of the current operation mode of the high-gap plant protection machine, and the current best driving mode is then

selected. The specific process is as follows:

In the first stage, the system self-test is successfully passed by the vehicle controller; if no serious fault is detected, then the plant protection machine is started[31]. The operating state of the vehicle is determined by the interaction between the vehicle and lifting device controllers[32,33].

In the second stage, the speed sensor is used to collect changes in the traveling speed of the plant protection machine in real time. The load torque that the vehicle must overcome is analyzed and predicted by the vehicle controller according to the collected information such as the speed and soil specific resistance. The load and target torque of the high efficiency range are then compared using the controller.

1) If the load torque T_f to be overcome is less than the target torque T_e (i.e., $T_f < T_e$), then it must be in the rear-drive mode which considers power and economy.

2) If the load torque T_f to be overcome is greater than the target torque T_e of the rear axle (i.e., $T_f > T_e$), then switching the mode and entering the four-wheel driven mode is necessary to ensure the power performance of the plant protection machine.

3) According to the real-time feedback sensor data of the system, when it is recognized that the planting machine try load torque T_f is less than the target torque T_e of the rear axle, (i.e., $T_f < T_e$), then the system is adjusted from 4WD mode to rear drive mode to reduce energy consumption.

where, T_f is the load torque, N·m; T_e is the target torque, N·m.

In the third stage, the angle change of the plant protection machine is collected by the angle sensor in real time, and the working condition of the vehicle is analyzed and calculated by the vehicle controller according to the collected information such as vehicle angle θ and soil specific resistance K_λ. The turning action in place is finally completed by the controller.

The overall mode switching process of the entire upland gap plant protection machine drive system is shown in Figure 3.

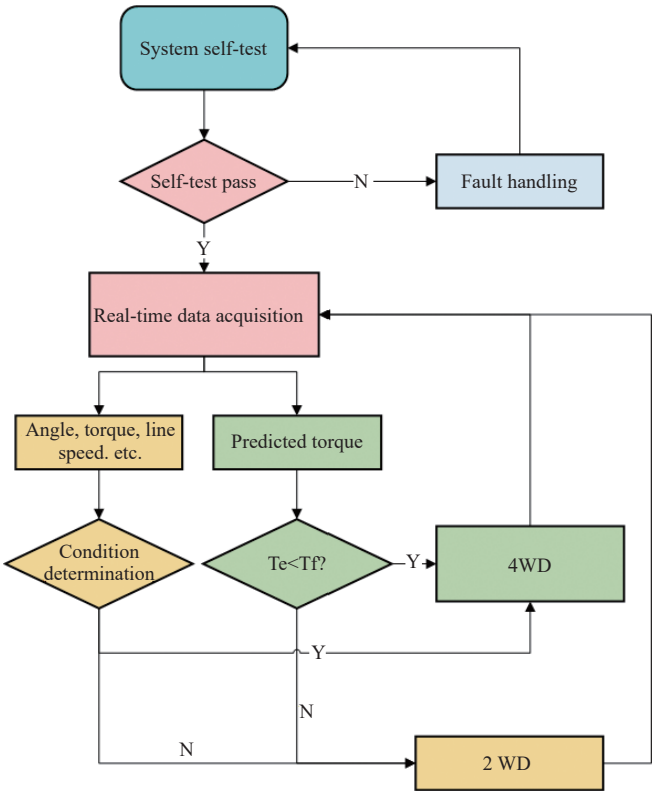

Figure 3 Mode switching process of the driver system

3.2 Timely four-wheel driven system torque distribution strategy

When the high-gap plant protection machine is in four-wheel driven mode, the torque of the front and rear axles should be distributed in accordance with the load torque that must be overcome by the plant protection machine as follows. First, the load torque of the plant protection machine is obtained in accordance with the method in Section 2. Then, combined with collected parameter estimation and vehicle signals, the vertical load ratio of front and rear axles[19,34], slip rate, and speed difference of front and rear axles are determined, and the layered control framework is set according to the performance requirements of timely four-wheel driven vehicles under different working conditions, as shown in Figure 4.

The hierarchical control framework is mainly divided into three parts: condition identification, feedback control and torque distribution[35,36]. The top layer recognizes the working conditions by monitoring the wheel angle, vehicle speed, pedal opening and other parameters to determine the working conditions of the machine, and transmits the relevant information to the middle layer. The middle layer formulates the control mode and determines the torque signal according to the operating conditions and transmits it to the bottom layer to provide the latter with specific control strategies. The bottom layer relies on sensor data and control algorithms to transform the strategy provided by the middle layer into the actual torque distribution scheme, thus realizing the precise control of vehicle power output. The organic combination of the three layers not only improves the stability and reliability of the system, but also ensures the high efficiency of the distribution strategy.

The electronically controlled clutch in the torque manager has two states: slip and lock. The switching logic of sliding and locking, where T_{cd} is the target torque value calculated based on dynamic friction, is shown in Figure 5.

The calculation of the locking critical torque T_{lock} is realized by identifying the clutch state, as shown in the sliding and locking switching logic in Figure 5. When the clutch is locked, the following relationship is demonstrated by the input and output angular speeds of the torque manager:

$$\dot{w}_f = \dot{w}_r \tag{6}$$

where, w_f is the torque manager input, rad/s; w_r is the output axial angular speed rad/s.

When the clutch is locked:

$$T_c = T_{\text{lock}} \tag{7}$$

According to the wheel dynamic balance equation:

$$T_{fl} - F_{zfl} fr - F_{xfl} r = I_{fl} \dot{w}_{fl} \tag{8}$$

$$T_{fr} - F_{zfr} fr - F_{xfr} r = I_{fr} \dot{w}_{fr} \tag{9}$$

$$T_{rl} - F_{zrl} fr - F_{xrl} r = I_{rl} \dot{w}_{rl} \tag{10}$$

$$T_{rr} - F_{zrr} fr - F_{xrr} r = I_{rr} \dot{w}_{rr} \tag{11}$$

where, T_{lock} is the critical torque locked by the torque manager, N·m; T_{fl}, T_{fr}, T_{rl}, T_{rr} are the driving torques of the front left, front right, rear left, and rear right tires, respectively, N·m; T_{xfl}, T_{xfr}, T_{xrl}, T_{xrr} are the longitudinal forces of the front left, front right, rear left, and rear right tires, respectively, N·m; T_{zfl}, T_{zfr}, T_{zrl}, T_{zrr} are the vertical loads of the front left, front right, rear left, and rear right tires, respectively, N·m; w_{fl}, w_{fr}, w_{rl}, w_{rr} are the angular speeds of

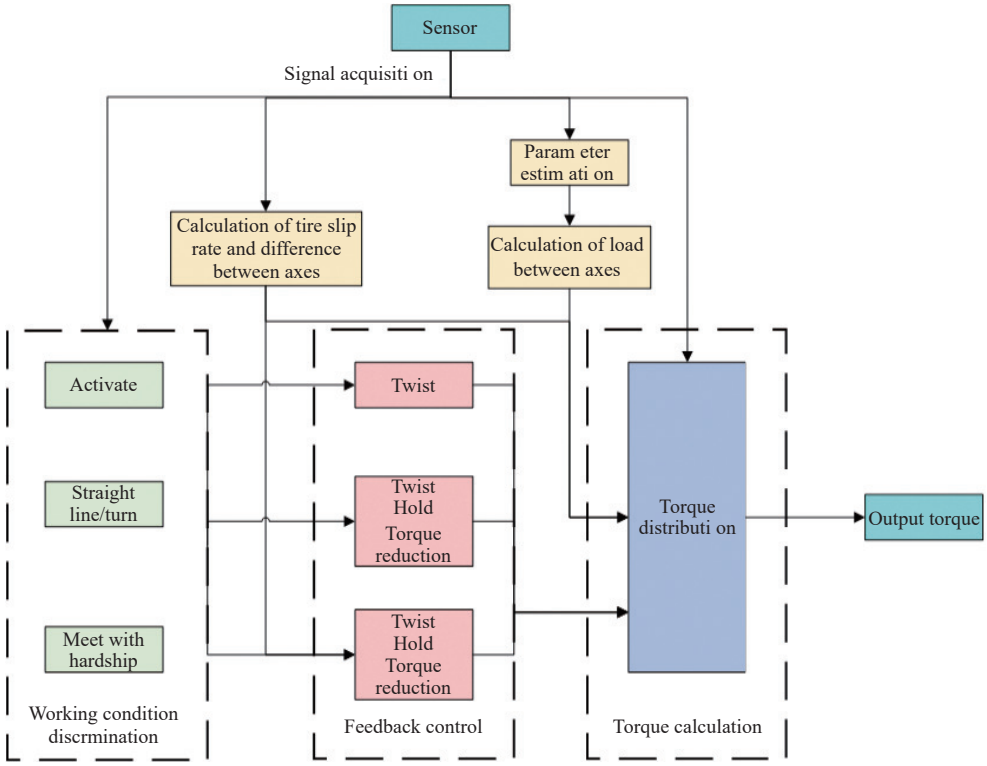

Figure 4 Hierarchical control frame diagram

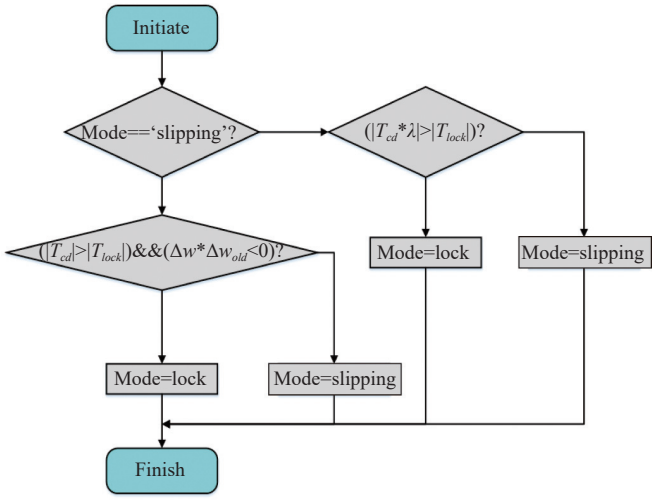

Figure 5 Switching logic of clutch friction plate sliding and locking

the front left, front right, rear left, and rear right tires, respectively rad/s; I_{fl}, I_{fr}, I_{rl}, I_{rr} are the moments of inertia of the front left, front right, rear left, and rear right tires, respectively, N·m.

The relationship of the front and rear axle drive torque is respectively shown as follows:

$$T_{fl} = T_{fr} = \frac{i_f T_0 - T_{\text{lock}}}{2i_f} \tag{12}$$

$$T_{rl} = T_{rr} = \frac{i_r T_{\text{lock}}}{2} \tag{13}$$

The angular velocity relation is:

$$w_f = \frac{w_{fl} + w_{fr}}{2i_f} \tag{14}$$

$$w_r = \frac{(w_{rl} + w_{rr})i_r}{2} \tag{15}$$

The difference in inertia of the four driving wheels is ignored.

$$I_{fl} = I_{fr} = I_{rl} = I_{rr} \tag{16}$$

Overall, the locking critical torque is:

$$T_{\text{lock}} = \frac{T_0 - (F_{zf} - F_{zr})fr - (F_{xf} - F_{xr})r}{2i_r} \tag{17}$$

The timely four-wheel driven torque distribution relationship when the clutch is in the slipping state (mode = slipping) is as follows:

$$T_f = T_0 - \frac{(T_c + I_{\text{axlef}}\dot{w}_r)}{i_f} \tag{18}$$

$$T_r = i_r(T_c - I_{\text{axler}}\dot{w}_r) \tag{19}$$

$$T_c = \text{sign}(w_f - w_r)|T_c| \tag{20}$$

where, I_{axlef}, I_{axler} are the moments of inertia of the front and rear axes of the torque manager, respectively, N·m.

When the clutch is in the locked state (mode = lock), the front and rear connection shafts of the four-wheel driven system are rigidly connected in time, and the torque transmission characteristics are related to the angular stiffness K_t of the connection shaft and the damping D_t. The front and rear torque distribution relationship is as follows:

$$T_f = T_0 - \frac{(T_{\text{torsion}} + I_{\text{axlef}}\dot{w}_f)}{i_f} \tag{21}$$

$$T_r = i_r(T_{\text{torsion}} - I_{\text{axlef}}\dot{w}_r) \tag{22}$$

$$T_{\text{torsion}} = K_t(\theta_f - \theta_r) + D_t(w_f - w_r) \tag{23}$$

where, T_{torsion} is the torsional torque of the drive train under locked condition, N·m.

4 Simulation analysis

4.1 Simulation model construction

In the simulation software, the simulation platform of the transmission system of the high-gap plant protection machine is

established. Torque/speed prediction, model predictive control, engine, battery, transmission, and longitudinal dynamics modules are included in the vehicle model, and the relationships among each module are shown in Figure 6.

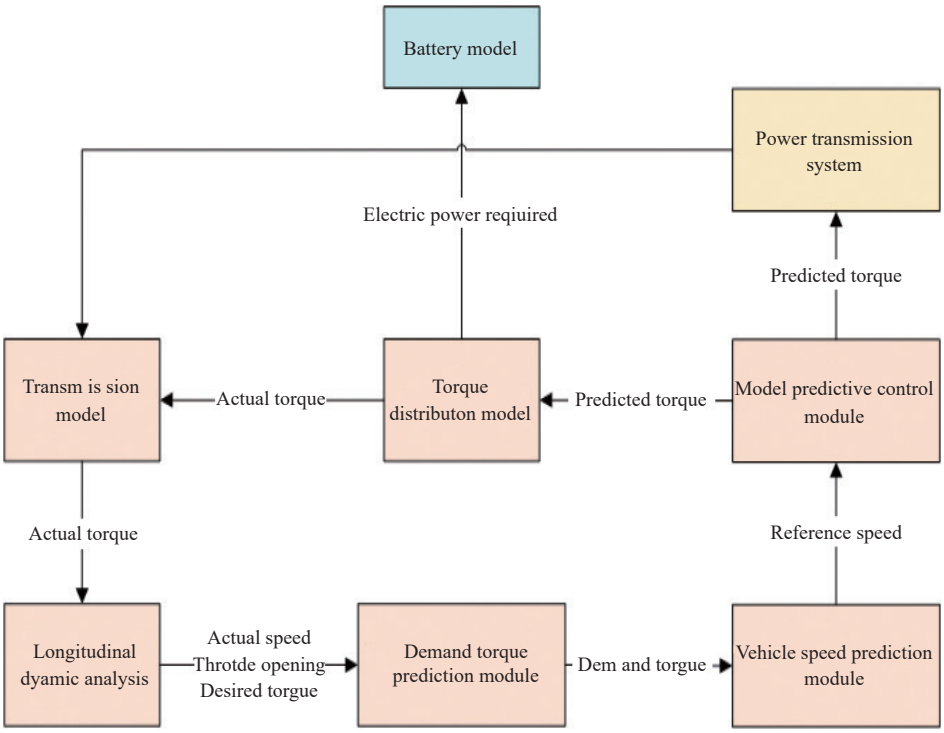

Figure 6 Schematic of vehicle model

The load torque calculation module is comprised by the following three parts: demand load torque acquisition, drive pattern recognition, and torque distribution modules. The calculation of demand load torque and the optimal torque distribution of the high-gap plant protection machine is realized by this module under different working conditions, as shown in Figure 7.

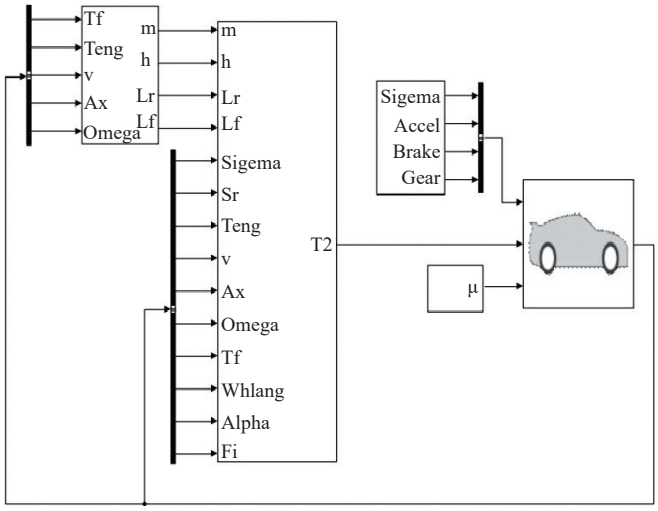

Figure 7 Torque distribution model

4.2 Simulation and analysis of straight-line driving conditions

Under different driving conditions, the torque distribution is adaptively adjusted by the timely four-wheel driven plant protection machine to improve the dynamic performance of the entire vehicle. The torque distribution strategy is then triggered only when the load torque overcome by the driving wheel is greater than the target torque in the straight-line driving process. The two-wheel driven state is used by the timely four-wheel driven plant protection machine under normal circumstances. Therefore, typical working conditions (timely four-wheel driven plant protection machine from high to low adhesion road surface) are designed, the data obtained under such working conditions are analyzed, and a conclusion is finally drawn.

When driving on the high to the low adhesion road surface, the static state is the starting point of the timely four-wheel driven plant protection machine, and the variable adhesion road surface is entered by the plant protection machine at 17 s. The adhesion coefficient of the road surface is changed from 0.6 of the high adhesion road surface to 0.2 of the low adhesion road surface. When the timely four-wheel driven plant protection machine is running in a straight line, the simulation curves of various parameters of the road surface from high to low adhesion plant protection machine are varied, as shown in Figures 8a-8d. In the starting stage of the plant protection machine, the top working condition is selected as the starting working condition, and the forward distribution torque is determined in accordance with the ratio of front and rear vertical loads. The forward distribution torque is extremely large at this time. However, the speed difference between the front and rear axle is zero, thereby meeting the driver's demand for rapid acceleration under the starting working condition. Moreover, the speed of the front and rear wheels is low, and the rolling radius difference between the front and rear wheels is small. At this time, the tire damage is low when the front and rear axle speed difference is zero. At 12.3 s, the vehicle speed is greater than 10 km/h, and the plant protection machine is changed from the starting condition to the straight-line driving condition.

In the straight-line driving condition, the speed difference between the front and rear axle is zero, indicating that the torque distributed to the front axle is excessively large; thus, the torque should be reduced. The forward torque should be gradually reduced in accordance with the set decline step. In addition, when the front torque is gradually decreased to zero, the rear wheel slip

rate is maintained within the range of the best slip rate, indicating a large road adhesion. The power demand of timely four-wheel driven plant protection machine under the rear-driven state is addressed by the longitudinal force provided by the rear wheel road, and the plant protection machine is changed from four- to two-wheel driven mode.

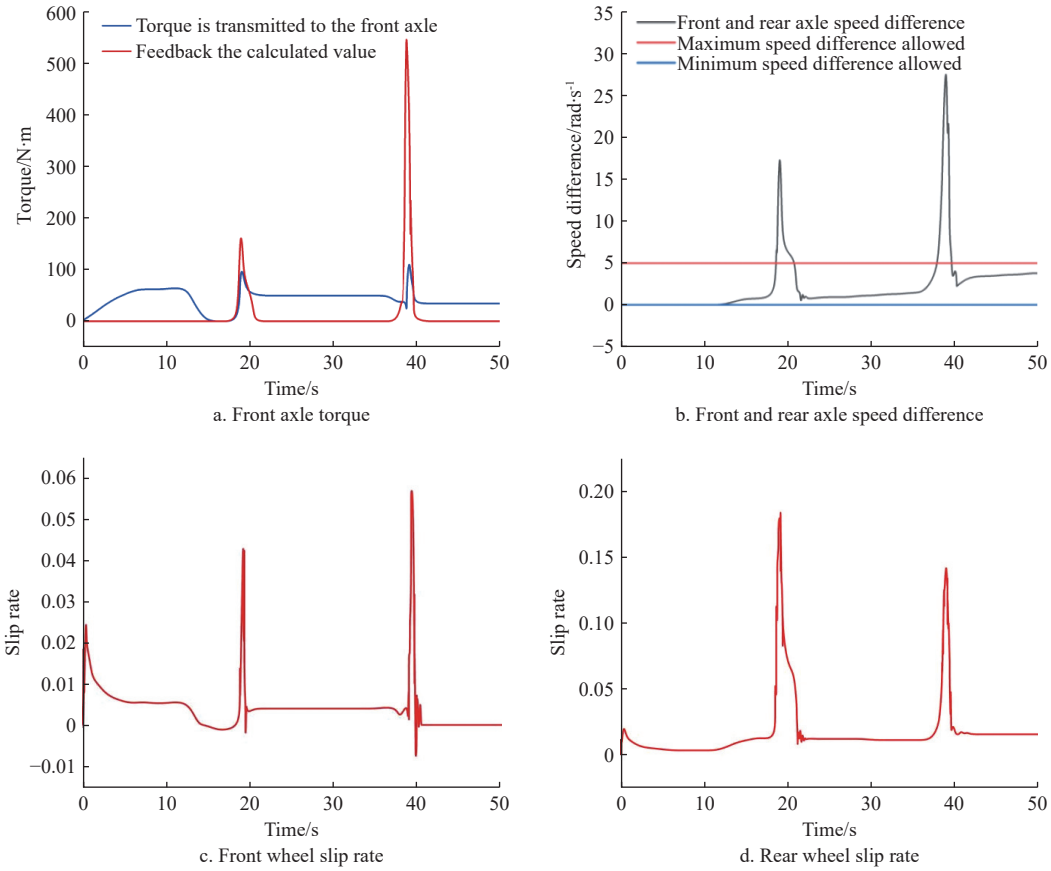

Figure 8 Linear condition simulation results

At 17 s, the high to the low adhesion road surface is traveled by the front wheel of the plant protection machine under the two-wheel driven state. The forward distribution torque is zero under the two-wheel driven state. Therefore, the front wheel slip rate is zero, and the front wheel speed remains unaffected by the road adhesion. The rotational speed difference between the front and rear wheels does not change significantly. When the rear wheel is driven from the high to the low adhesion road surface, the front and rear wheels are in the low adhesion road surface. Under the same slip rate, the longitudinal force provided by the rear wheel road surface will also decrease, and the slip rate of the rear wheel will increase, gradually extending the speed difference between the front and rear axle. When the rear wheel slip rate is increased to 0.18 and the optimal slip rate is exceeded, the plant protection machine is changed from the two-wheel driven to the four-wheel driven state, and the torque is slowly increased forward. The size of the increased torque is determined by the feedback based on the ratio of front and rear loads and the speed difference between the front and rear axles. The actual forward transmitted torque is gradually increased in accordance with the set step length until it coincides with the calculation curve of feedback. The speed difference between front and rear is controlled within the allowable range, and the current forward output torque is maintained. When the set threshold is exceeded by the plant protection machine at 17 s in the holding stage, the forward output torque is decreased in accordance with the step length, the rear torque is increased, and the speed difference between the front and back is extended. In the process of forward output torque reduction, the rear wheel slip rate is increased to approximately 0.14, the optimal slip rate is exceeded, and the forward transfer torque is not zero at this time. This condition indicates that the road adhesion is low at this time, and the power demand of the current plant protection machine cannot be addressed by the adhesion force provided by the rear wheel road surface. Moreover, the forward transfer torque is increased to the calculated value of feedback by step length. The rear wheel slip rate is controlled back to the best slip rate range, and the speed difference between the front and rear axles is maintained within the allowable range.

4.3 Simulation analysis of turning conditions

The timely four-wheel driven plant protection machine was set to start from the static state with a 0.06 road surface adhesion coefficient to reflect the influence of torque distribution on lateral stability. The plant protection machine was driven in the two- and four-wheel driven states based on the turning control strategy during the turning process after 12.8 s. The simulation results were then compared and analyzed, and a conclusion was drawn.

The timely four-wheel driven plant protection machines were driven in the two- and four-wheel driven states based on the turning control strategy under the above turning conditions, and the speed changes in the plant protection machines are shown in Figures 9. If the plant protection machine turns in the two-wheel driven state, then the speed difference between the front and rear axle rapidly increases, and the yaw speed shifts to −0.6 rad/s, resulting in side-sliding and tail dumping and reducing the speed. In this case, the risk of poor lateral stability is substantial, as shown in Figure 10.

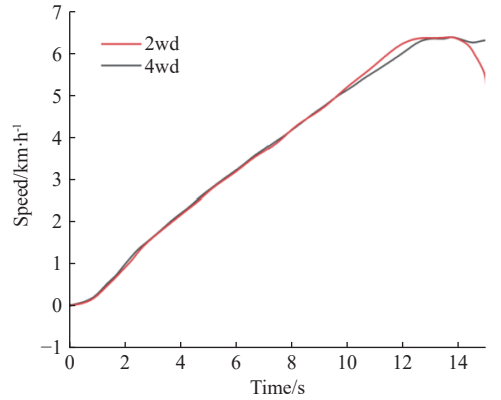

Figure 9 Curve of speed change in different states

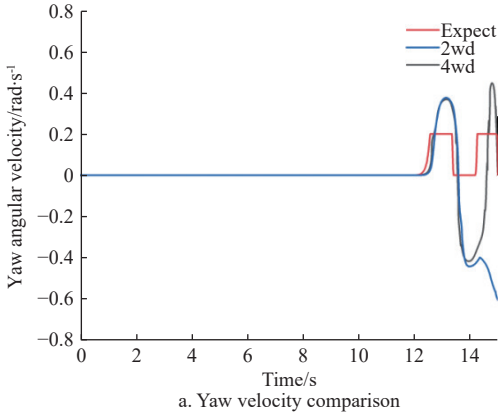

a. Yaw velocity comparison

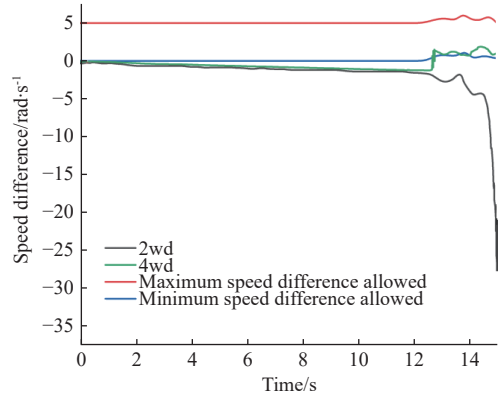

b. Front and rear axle speed difference

Figure 10 Simulation results of turning condition

When the timely four-wheel driven plant protection machine is turned based on the turning control strategy after 12.8 s, the machine enters the feedback adjustment control based on the speed difference between the front and rear axle because the speed difference between these axes is outside the permissible range. The forward distributed torque is then gradually changed to the target value according to the set step length and the torque signal output value, and the speed difference between the front and rear is stable at 1 rad/s. The figure shows that the value is maintained within a reasonable range. The actual yaw speed peak value of 0.46 rad/s for a timely four-wheel driven vehicle equipped with a turning control strategy is lower than that of 0.6 rad/s for a rear-drive vehicle. The trend of the actual yaw speed is similar to that of the ideal yaw speed, and the difference between the actual and ideal yaw speeds is small in the entire process. This value is close to the ideal turning state, wherein tail dumping is absent and the stability is higher than that of the rear-drive plant protection machine.

Overall, when the timely four-wheel driven plant protection machine is driving in turning conditions, the incremental feedback control on the rotational speed difference of the front and rear shafts is conducted in accordance with the torque distribution strategy formulated in this paper. Compared with the rear-drive plant protection machine, the lateral stability of this machine can be effectively improved. The feasibility of the formulated torque distribution strategy in turning conditions is verified on the basis of these results.

5 Whole vehicle test

5.1 Straight line driving test

The dynamic performance of four-wheel driven vehicles equipped with four-wheel driven controllers is verified using the linear working condition test. Therefore, the main vehicle dynamic test project is conducted to assess the evaluation indicators of dynamic performance. The rapid acceleration start tests of low and high to low adhesion road surfaces are performed in this paper to investigate the vehicle dynamics after control.

The torque distributor is opened or closed in advance according to the test requirements, while all four wheels of the plant protection machine are pressed on the road and maintained at rest, as shown in Figure 11.

Figure 11 Straight line driving test diagram

When the test personnel are ready, the plant protection machine is driven in a straight line on the low adhesion road surface. As shown in Figure 12a, the peak longitudinal acceleration of the plant protection machine is only 0.26 m/s² under the two-wheel driven condition and its average longitudinal acceleration is approximately 0.17 m/s², as visually demonstrated by the comparison of longitudinal acceleration signals in the rapid acceleration start test on low adhesion road surface. Meanwhile, the peak longitudinal acceleration of the plant protection machine under the four-wheel driven condition can reach 0.51 m/s². The average longitudinal acceleration reaches approximately 0.30 m/s². The comparison results of longitudinal acceleration show that the dynamic performance of the four-wheel driven plant protection machine is superior to that of the two-wheel driven plant protection machine. The effectiveness and feasibility of the longitudinal control strategy in the four-wheel driven control strategy in this paper are also verified by the test results.

The comparison results of the longitudinal acceleration curve in the rapid acceleration start test on the high to low adhesion road surface revealed minimal differences in longitudinal acceleration between the four- and two-wheel driven modes within the range of 0.8-2.2 s, as shown in Figure 12b. That is, when the plant protection machine has not entered the low adhesion road surface, the peak

longitudinal acceleration was approximately 0.48 m/s^2. However, when the plant protection machine began to enter the low adhesion road surface (that is, after 2.2 s), the average longitudinal acceleration of the plant protection machine in the four-wheel driven mode was approximately 0.28 m/s^2, while that of the plant protection machine in the two-wheel driven mode was only approximately 0.12 m/s^2. The power performance of the four-wheel driven mode was superior to that of the two-wheel driven mode.

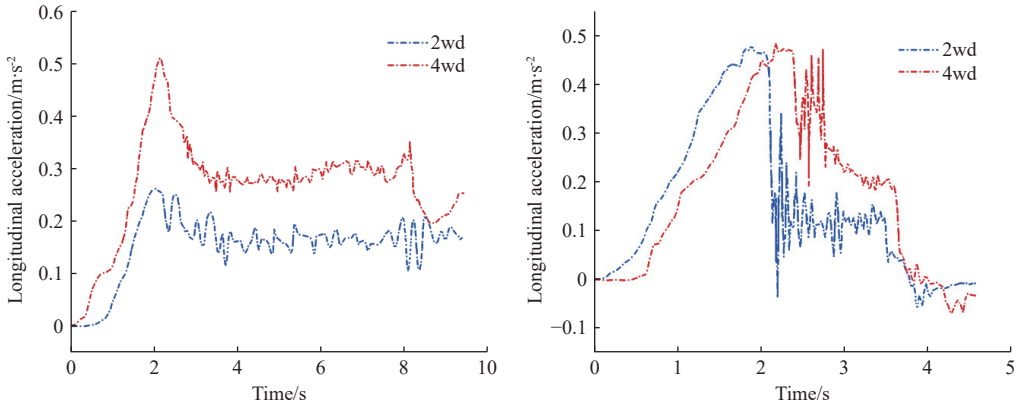

a. Low adhesion longitudinal acceleration signal b. Variable adhesion longitudinal acceleration signal

Figure 12 Straight-line driving test results

5.2 Turning driving test

As shown in Figure 13, the initial speed of the plant protection machine is 6 km/h in the single-line shifting condition. The front wheel angle is transformed into sinusoidal input turning condition test after driving for 2 s.

Figure 13 Turning driving test diagram

As shown in Figure 14a, a large deviation from the expected value of up to 0.73 rad/s is demonstrated by the yaw velocity and side deflection angle of the center of mass of the plant protection machine under the single-line shifting condition in the absence of control. The expected value cannot be successfully tracked, and a stable state can be reached after a long time.

Figure 14b shows that the maximum side deflection angle of the center of mass can reach 4.13°, at which time the plant protection machine almost loses stability. This phenomenon easily causes the driver to panic and produces further misoperation, and a large deviation is displayed by the driving trajectory of the car. After the control is applied, the yaw speed of the plant protection machine can successfully follow the expected value, the maximum is 0.61 rad/s, the side deflection angle of the plant protection machine is restrained, and the side deflection angle of the center of mass is not more than 2.8°. The plant protection machine can effectively follow the intentions of the driver, travel according to the ideal trajectory, and improve the lateral stability of the plant protection machine. The results show that the torque distribution control strategy can maintain the lateral stability of the plant protection machine during lane changing at high speed.

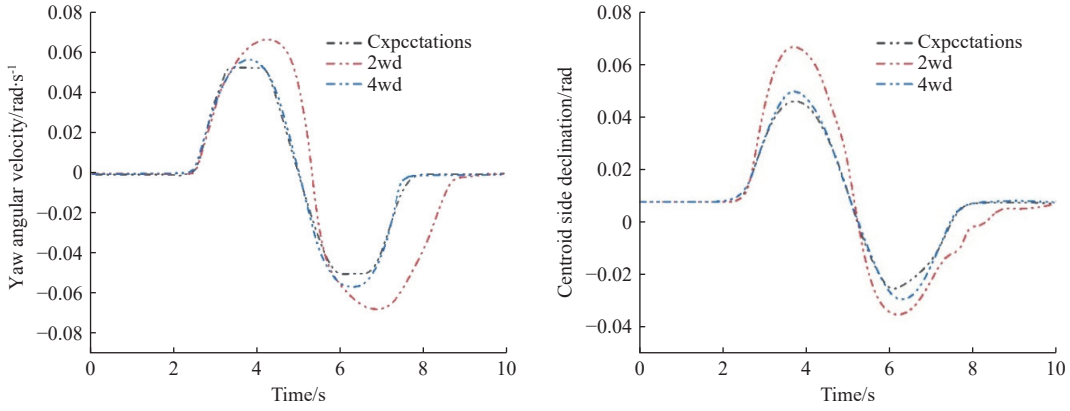

a. Yaw angular velocity b. Lateral deflection angle of center of mass

Figure 14 Turn driving result

6 Conclusions

Taking the timely four-wheel driven system of the high-gap plant protection machine as the object in this study, the load torque of this machine was analyzed under several typical working conditions, the selection of the vehicle drive mode under different working conditions was emphasized, the torque distribution under the timely four-wheel driven mode was examined, and an effective

control strategy was formulated. The following conclusions were obtained through simulation analysis:

1) A layered control framework was established. In this framework, the top layer was used for working condition identification, the middle layer was for torque signal determination and control mode selection, and the bottom layer was for torque calculation. The corresponding torque distribution strategy between shafts was formulated in accordance with the performance requirements under different working conditions.

2) Tire skid was effectively avoided, road adhesion was utilized, and vehicle power was improved using the formulated control strategies of the starting and straight-line driving conditions. The lateral stability of vehicles was efficiently enhanced by the control strategy by the turning condition.

3) The simulation verification of the drive system revealed that the power components of the entire drive system can successfully work together. The working characteristics of the high-gap plant protection machine in various modes were reflected by the aforementioned findings, and the drive mode switching control strategy and torque distribution were found to be reasonable and effective under different working conditions.

Acknowledgements

The research is funded partially by the Agricultural Science and Technology Independent Innovation Fund of Jiangsu Province (Grant No. CX(22)3101), the National Key R&D Program (Grant No. 2022YFD2001204), and the International Science and Technology Cooperation Project of Jiangsu Province (Grant No. BZ2022002), the Natural Science Foundation of Jiangsu Province (Grant No. BK20210407).

[References]

[1] Ge A L, Guo L S, Zhang T. Study of electronically controlled optimal torque distribution system for 4WD. Transactions of the CSAM, 2002; 33(6): 16–19. (in Chinese)

[2] Wang Y J, Yang F Z, Pan G T, Liu H Y, Zhang J Q. Design and testing of a small remote-control hillside tractor. Transactions of the ASABE, 2014; 57(2): 363–370.

[3] Sun C, Nakashima H, Shimizu H, Miyasaka J, Ohdoi K. Physics engine application to overturning dynamics analysis on banks and uniform slopes for an agricultural tractor with a rollover protective structure. Biosystems Engineering, 2019; 185: 150–160.

[4] Qi W C, Li Y M, Zhang J H, Qin C J, Liu C L, Yin Y P. Double closed loop fuzzy PID control method of tractor body leveling on hilly and mountainous areas. Transactions of the CSAM, 2019; 50(10): 17–23, 34. (in Chinese)

[5] Geng A J, Zhang M, Zhang J, Zhang Z L, Gao A, Zhen J L. Design and experiment of automatic control system for corn header height. Transactions of the CSAM, 2020; 51(S2): 118–125. (in Chinese)

[6] Janulevicius A, Juostas A, Pupinis G. Estimation of tractor wheel slippage with different tire pressures for 4WD and 2WD driving systems. Engineering for Rural Development, 2019; 22(96): 88–93.

[7] Hayat S, Ahmed S, Tanveer-ul-Haq, Jan S, Mehtab Q, Zeeshan N, et al. Hybrid control of PV-FC electric vehicle using Lyapunov based theory. International Journal of Advanced Computer Science and Applications, 2019; 10(10): 539–549.

[8] Piyabongkarn D, Lew J Y, Rajamani R, Grogg J A. Active driveline torque-management systems. IEEE Control Systems Magazine, 2010; 30(4): 86–102.

[9] Li B, Goodarzi A, Khajepour A, Chen S, Litkouhi B. An optimal torque distribution control strategy for four-independent wheel drive electric vehicles. Vehicle System Dynamics, 2015; 53(8): 1172–1189.

[10] Arash M, Basilio L, Aldo S, Patrick G, Saber F, Jasper D. A fast and parametric torque distribution strategy for four-wheel-drive energy-efficient electric vehicles. IEEE Transactions on Industrial Electronics, 2016; 63(7): 4367–4376.

[11] Cao K B, Hu M H, Wang D Y, Qiao S P, Guo C, Fu C Y, et al. All-wheel-drive torque distribution strategy for electric vehicle optimal efficiency considering tire slip. IEEE Access, 2021; 9: 25245–25257.

[12] Yan X, Zhang H, Li X, Li Y, Xu L. Control strategy of torque distribution for hybrid four-wheel drive tractor. World Electric Vehicle Journal, 2023; 14(7): 190.

[13] Peng B, Zhang H, Xuan F, Xiao W. Torque distribution strategy of electric vehicle with in-wheel motors based on the identification of driving intention. Automotive Innovation, 2018; 1: 140–146.

[14] Chen LQ, Tan YD, Wu R, Miao W, Hu F. Torque distribution control strategy of electronically controlled four-wheel drive axle based on genetic algorithm. Transactions of the CSAM, 2017; 48(7): 361–367.

[15] Wong A, Kasinathan D, Khajepour A, Chen S, Litkouhi B. Integrated torque vectoring and power management framework for electric vehicles. Control Engineering Practice, 2016; 48: 22–36.

[16] Novellis D, Sorniotti A, Gruber P. Wheel torque distribution criteria for electric vehicles with torque-vectoring differentials. IEEE Transactions on Vehicular Technology, 2013; 63(4): 1593–1602.

[17] Lee H. Four-wheel drive control system using a clutchless centre limited slip differential. Proceedings of the Institution of Mechanical Engineers, Part D: Journal of Automobile Engineering, 2006; 220(6): 665–681.

[18] Wang J H, Wang Y C, Fu T J, Zhang B S. A study on the effect of torque sensing LSD on the handling and stability of a RWD vehicle. Automotive Engineering, 2006; 28(5): 460–464, 476.

[19] Zhou D, Hou P, Xin Y, Lv X, Wu B, Yu H, et al. Study on the control of torque distribution of 4wd corn harvester operation drive. Applied Sciences, 2021; 11(19): 9152.

[20] Wheals J C, Deane M, Drury S, Griffith G, Harman P, Parkinson R, et al. Design and simulation of a torque vectoring™ rear axle. SAE Technical Paper, 2006; 2006-01-0818.

[21] Hancock M, Williams R, Gordon T, Best M. A comparison of braking and differential control of road vehicle yaw-sideslip dynamics. Proceedings of the Institution of Mechanical Engineers, Part D: Journal of Automobile Engineering, 2005; 219(3): 309–327.

[22] Bianchi D, Borri A, Di Benedetto MD, Di Gennaro S, Burgio G. Adaptive integrated vehicle control using active front steering and rear torque vectoring. International Journal of Vehicle Autonomous Systems, 2010; 8(2-4): 85–105.

[23] Jalali M, Hashemi E, Khajepour A, Chen S, Litkouhi B. Integrated model predictive control and velocity estimation of electric vehicles. Mechatronics, 2017; 46: 84–100.

[24] Suzuki R, Ikeda Y. Driving/braking force distribution of four wheel vehicle by quadratic programming with constraints. In 49th IEEE Conference on Decision and Control (CDC), IEEE, 2010; pp.4882–4889.

[25] Didikov R, Dobretsov R, Galyshev Y. Power distribution control in the transmission of the perspective wheeled tractor with automated gearbox. Energy Management of Municipal Transportation Facilities and Transport. Cham: Springer International Publishing, 2017; 192–200.

[26] Wong J Y. Theory of ground vehicles. John Wiley & Sons, 2022.

[27] Middleton N. The global casino: an introduction to environmental issues. Routledge, 2018.

[28] Yao Q, Tian Y. A model predictive controller with longitudinal speed compensation for autonomous vehicle path tracking. Applied sciences, 2019; 9(22): 4739.

[29] Gim G. An analytical model of pneumatic tyres for vehicle dynamic simulations. Part 2: Comprehensive slips. International Journal of Vehicle Design, 1991; 12(1): 19–39.

[30] Gim G, Nikravesh P E. An analytical model of pneumatic tyres for vehicle dynamic simulations. Part 3: Validation against experimental data. International Journal of Vehicle Design, 1991; 12(2): 217–228.

[31] Gim G, Nikravesh P E. An analytical model of pneumatic tyres for vehicle dynamic simulations. Part 1: Pure slips. International Journal of Vehicle Design, 1990; 11(6): 589–618.

[32] Ohba M, Suzuki H, Yamamoto T, Takuno H. Development of a new electronically controlled 4WD system: Toyota active torque control 4WD. SAE Transactions, 1999; 1999-01-0744.

[33] Hu J J, Liu H, He Z B. Effect of drive force distribution control on vehicle steering driving stability. China Journal of Highway and Transport, 2013; 26: 183–190.

[34] Hancock M J, Williams R A, Fina E, Best M C. Yaw motion control via active differentials. Transactions of the Institute of Measurement and Control, 2007; 29(2): 137–157.

[35] Park J, Jang I G, Hwang S H. Torque distribution algorithm for an independently driven electric vehicle using a fuzzy control method: Driving stability and efficiency. Energies, 2018; 11(12): 3479.

[36] Feng N L, Zheng M Q, Ma B. Dynamic performance simulation of power shift clutch during shift. Journal of Beijing Institute of Technology, 2000; 9(4): 445–450.